



SYNTHESIS AND CHARACTERIZATION OF GOLD NANOPARTICLES USING CEFOTAXIM SODIUM AND ITS SCHIFF BASE DERIVATIVE WITH 4-N,N-DIMETHYLAMINO BENZALDEHYDE AS REDUCING AND STABILIZING AGENTS

Ahlam Jameel Abdulghani*, Rasha Kudher Hussain

Chemistry Department, College of Science, Baghdad University, Baghdad, Iraq

*Corresponding author,

Email: ahlamjameel@scbaghdad.edu.iq

ABSTRACT

Conjugated GNPs were synthesized by one step reaction of AuCl_4^- with cefotaxim (CFX) and its Schiff base derivative with 4-N,N-dimethylamino benzaldehyde [sodium 3-(acetoxymethyl)-7-((2Z)-2-(2-(4-dimethylamino) benzylideneamino) thiazol-4-yl)-2-(methoxyimino) acetamido)-8-oxo-5-thia-1-azabicyclo[4.2.0]oct-2-ene-2-carboxylate] (SCFX) without the need of reducing and functionalizing agents. The reduction process was monitored by uv-visible spectrophotometry and the synthesized GNPs were characterized by TEM, SEM, AFM and XRD analysis. The conjugation of GNPs with the two ligands was characterized by FTIR spectrophotometry. The size, morphology, and stability of GNPs were varied with concentration ratio of ligand/Au(III), pH medium and reaction temperature

Keywords: -Gold nanoparticles; cefotaxim; Schiff base; AFM; TEM,



Council for Innovative Research

Peer Review Research Publishing System

Journal: Journal of Advances in Chemistry

Vol. 11, No. 8

editorjaonline@gmail.com, www.cirjac.com



INTRODUCTION

Several methods have been reported to conjugate anti-biotics with GNPs [1-6]. Highly surface area of nanoparticles increases drug density on the surface and allows higher concentrations of drug or multiple drugs loaded on single particles [7, 8]. The Synthesis of GNPs can be proceeded in a one-step reaction where the antibiotic act as a reducing and functionalizing agent to afford the antibiotic- functionalized nanomaterial without using any linkers [4-6]. Cephalosporins are β - lactam antibiotics which are based upon the four-membered nitrogen-containing beta-lactam ring that gives these agents their antibacterial activity. Stable GNPs were synthesized by one step reaction using different cephalosporin antibiotics such as cephalexin, cefaclor, [3] ciproflaxin [1], and ceftriaxone[1] as a stabilizing agents in presence of reducing agent. As a primary amine group carriers, some of these drugs acted as both reducing and capping agent for the synthesis of gold nanoparticles[1-3,7]. Accordingly, condensation of the free amino group of β -lactam antibiotics with different carbonyl compounds to form Schiff bases may inhibit the reduction of Au(III) ions. In this paper, we describe a single one pot synthesis of gold nanoparticles using the β -lactam antibiotic, cefotaxim, (CFX) compared with its Schiff base derivative [sodium 3-(acetoxymethyl)-7-((2Z)-2-(2-(4-dimethylamino) benzylideneamino) thiazol-4-yl)-2-(methoxyimino) acetamido)-8-oxo-5-thia-1-azabicyclo[4.2.0]oct-2-ene-2-carboxylate] (SCFX) in aqueous solutions without the addition of reducing and dispersing agents.

The reduction process was pursued by uv-visible spectrophotometry at different conditions like concentration ratio of reactants, pH and temperature. The synthesized GNPs were characterized by uv-visible spectrophotometry, transmission electron microscopy (TEM), scanning electron microscopy (SEM), atomic force microscopy (AFM) and by X-ray diffraction (XRD) analysis

2. EXPERIMENTAL

2.1. Instrumentation

Electronic spectra in the (UV-Visible) region (200-1100) nm were recorded on SHIMADZU 1650 UV-Visible spectrophotometer. FTIR spectra were recorded on Shimadzu FT-IR 8400S Fourier transform using KBr and CsI discs. TEM images were acquired using Philips CM10 Transmission electron microscope. Samples for TEM studies were prepared by placing a drop of the gold colloidal solution on a carbon coated copper grid which was dried under vacuum. SEM images were acquired using TE SCAN VEGA III, Czech. Scanning electron microscope. AFM images were acquired using AFM model AA 3000 SPM 220 V-Angstrom Advanced INC. USA. Samples were prepared by applying few drops GNP solutions on a glass slide and a thin layer was formed as uniform as possible followed by vacuum drying. X-Ray diffraction (XRD) measurements were performed using a Shimadzu XRD-6000 x-ray diffraction spectrometer. All GNPs solutions were dialyzed prior to analysis by using a cellulose tube (MW cutoff 12 400 D) against 1 L of DDW for 9 h at 30 °C. Separation of nanoparticles was achieved by centrifugation CENTERFUGE C 41 7800 14000 r.p.m., Jouan, (France).

2.2. Materials and methods

All the following chemicals were of analytical grades and were used as received from suppliers: Cefotaxime Sodium $C_{16}H_{16}N_5O_7S_2Na$ GMBH, sodium chloroaurated dihydrate $NaAuCl_4 \cdot 2H_2O$ (Analar BDH), potassium hydrogen phthalate $2-(HO_2C)C_6H_4CO_2K$, 99.95% (BDH), potassium chloride, potassium dihydrogen orthophosphate KH_2PO_4 , and dipotassium hydrogen orthophosphate 99% (Analar). The Schiff base ligand SCFX was prepared before and the structural characterization of the compound was reported in our previous work [8]. Standard solutions of cefotaxime sodium salt ($C_{16}H_{16}N_5O_7S_2Na$, 2×10^{-4} M), and SCFX (1.6×10^{-3} M) were prepared by dissolving 0.1000 g of each reactant in 100 mL deionized water (DDW) in 100 mL volumetric flask to give the antibiotic stock solution. Then 10 mL of the stock solution was diluted to 100 mL with (DDW) in a 100 mL volumetric flask. A stock aqueous solution of $AuCl_4^-$ (5×10^{-3} M) was prepared by dissolving 0.1000 g of $NaAuCl_4 \cdot 2H_2O$ in 50 mL DDW in a volumetric flask. A standard solution of $AuCl_4^-$ (5×10^{-4} M) which contains (2.5×10^{-4} M) of Au^{3+} ions, was prepared by diluting 10 mL of the stock solution to 100 mL with (DDW).

Synthesis of gold nanoparticle conjugates

To different volumes of $AuCl_4^-$ standard solutions (5×10^{-4} M) : (0.25, 0.5, 0.75, 1.0, 1.25, 1.5, 2.0, 2.5, 3.0, and 3.5 mL) in ten 5 mL volumetric flasks were added one mL aliquots of standard solution (2 and 1.6×10^{-4} M) of each of cefotaxime and SCFX respectively with continuous stirring. The volumes were then completed to 5 mL by DDW, and the absorbance of each solution was measured at room temperature at different time intervals. To study the effect of pH the synthesis of GNPs was carried out at different pH (2.4, 2.89, 3.84, 4.85, 5.8, 6.92, 7.55, 8.92, 9.9, 10.9, 11.9). To study

the effect of temperature on the synthesis of GNPs by each ligand each set of solutions was heated for 5 minutes at (30, 40, 50, 60, 70 and 80 °C) for 5 min, in water bath with continuous stirring. The effect of heating periods on the synthesis rate of GNPs were studied by heating each sample at the selected temperature for (5, 10, 15, 20, 25,30, 45, 60) min.

3. RESULTS AND DISCUSSION

The UV–visible spectra of cefotaxime (CFX), SCFX and AuCl₄⁻ solutions as well as GNP solutions prepared from mixing equal volumes of standard aqueous solutions of AuCl₄⁻ (III) with each ligand at room temperature are shown in (Figure 1). The spectrum of AuCl₄⁻ solution exhibited a high intensity band at λ 240 nm and with a shoulder λ 290 nm assigned to LMCT transitions of tetrachloroaurate complex [9,10]. The spectrum of the (CFX) antibiotic (Figure 1A)) displayed a multiplet covering the uv region at wavelength range 200-300 nm with three absorption maxima at λ 238, 259 and 297 nm assigned to the π→π* transition [11]. The spectrum of SCFX in DDW (Figure 1B) displayed a multiplet band with three absorption peaks located at λ_{max} 235, 295, and 342nm attributed to the π→π* transition and a low intensity band observed at λ_{max} 430 nm refers to the n→π* transition[11].The solution mixtures of AuCl₄⁻ with the two ligands showed pink red colors and their spectra exhibited single absorption bands at λ_{max} 531and 532 nm respectively, indicating the reduction of AuCl₄⁻by the two ligands to form GNPs. The time required for the development of the pink color was 2 and 3.5 h for SCFX andCFX respectively

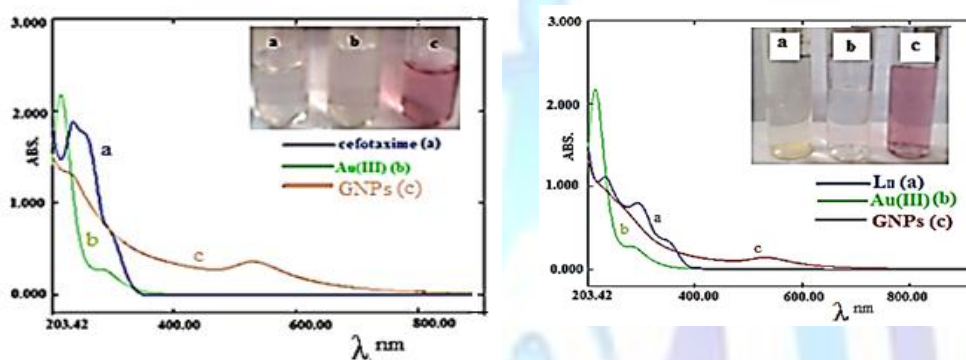


Figure 1. The UV-visible spectra and images of a- cefotaxime b- AuCl₄⁻ and c-synthesized gold nanoparticle in aqueous solutions after 24 h.

No additional bands were observed in the visible or NIR region which refers to the formation of spherical gold nanoparticles[12-20]. The proposed mechanism suggests that formation of GNPs may have proceeded through the oxidation of the amine of the aromatic thiazole ring from which the formed electrons go on to reduce the auric(III) ions to gold atoms according to the literature[21,22]. Cefotaxim molecules contain many active groups such as amino, amido, thio and carboxyl groups, which react easily with GNPs by chelation [23]. Furthermore, Cefotaxime molecules themselves, like many beta lactam drugs, can bind each other through van der Waals interaction and hydrogen bonding [24]. Ultimately, assemblies are made up of nanogold cores and the surrounding cefotaxime molecules. The higher capability of the Schiff base ligands SCFX to reduce the Au(III) ions to GNPs compared with CFX indicates the presence of additional site for electron donation or for further stabilization of GNPs like the azomethine group. It also proves that the reduction process by (CFX) is not attributed to amino group of thiazole ring only, but other electron donor sites at the beta lactam ring, amide group moiety as well as thio and carboxyl groups, at the thiazine ring are involved in the reduction process and chelation with GNPs[25].

3.1. Characterization of prepared gold nanoparticles

The size, morphology and surfaces of the synthesized gold nanoparticles were investigated by SEM, TEM and AFM analysis of GNPs. The TEM analysis of the cefotaxime conjugated GNPs showed that the particles were spherical in shape with smooth surface morphology and mono-dispersed in nature with narrow size distribution and mean size diameters of around 17 nm (Figures2).The SEM images and size distribution for cefotaxime and SCFX conjugated GNPs (Figures3 and 4 respectively) showed spherical nanoparticles with average size diameters around 60 and 27 nm respectively which indicates the difference in stabilizing effect between the two ligands. However the AFM images (Figures5 a and b respectively) showed the opposite result as the GNPs were spherical in shape and the average particle diameters were around 56 and 66 nm, respectively, which may be attributed to different sample preparation conditions that caused the formation of agglomerates.

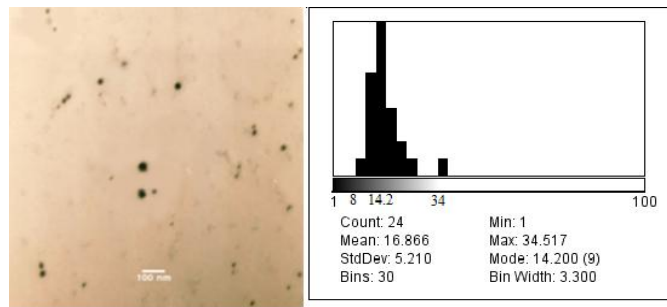


Figure2. TEM image and particle size distribution for CFX- GNPs conjugates.

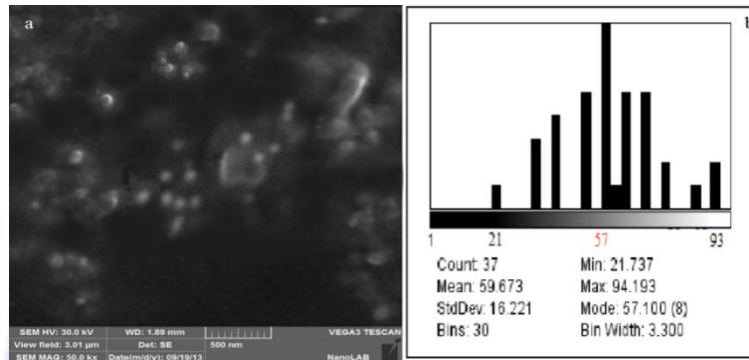


Figure 3.a-SEM image b-particle size distribution of the cefotaxime- synthesized GNPs (average particle size diameter= 60 nm)

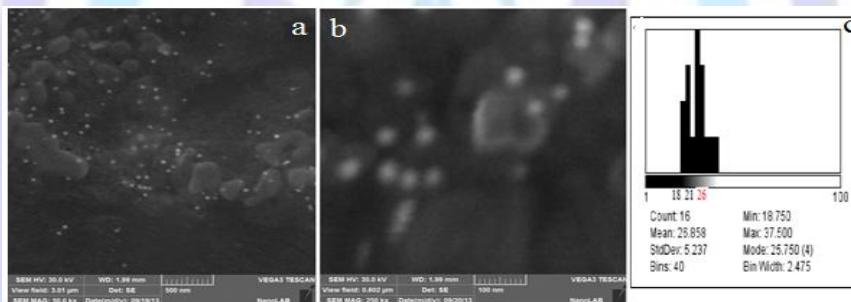


Figure4.a-SEM image b- cross section image and c-particle size distribution of the SCFX synthesized GNPs with an average size diameter 27 nm

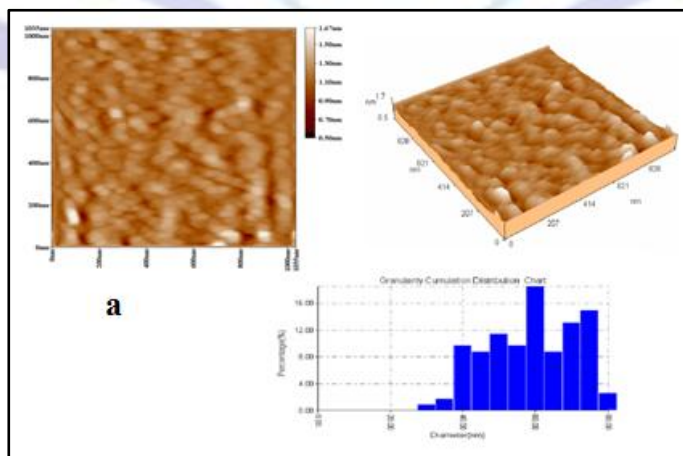


Figure 5a.AFM images and particle size distribution charts of the cefotaxime--synthesized GNPs with an average diameter around 56.47

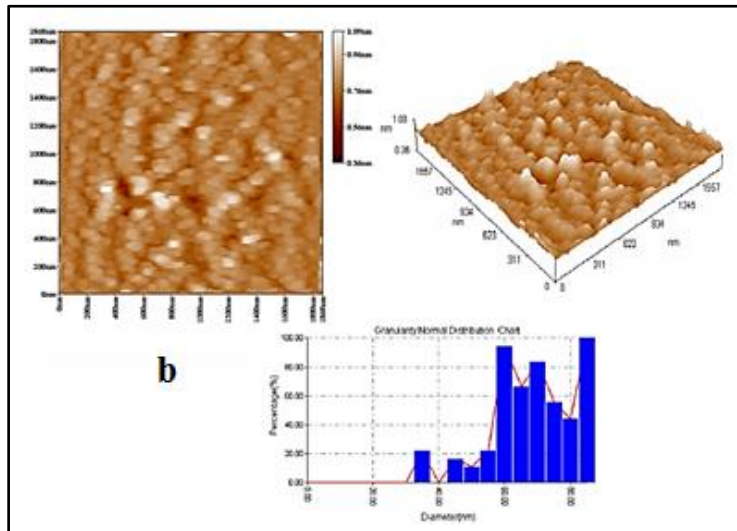


Figure 5b. AFM images and particle size distribution charts of the SCFX- synthesized GNPs with an average diameter around 66.17 nm

The XRD patterns of GNPs synthesized by cefotaxime and SCFX are shown in (Figures 6a and b)), respectively. Two diffraction peaks were observed at $2\theta = (38.0547, 44.531)$, and $(38.077, 44.42)$ degrees for the two samples respectively corresponding to the planes (111) and (200) of facecentered cubic (fcc) Au metal crystal lattice [12,19,26].

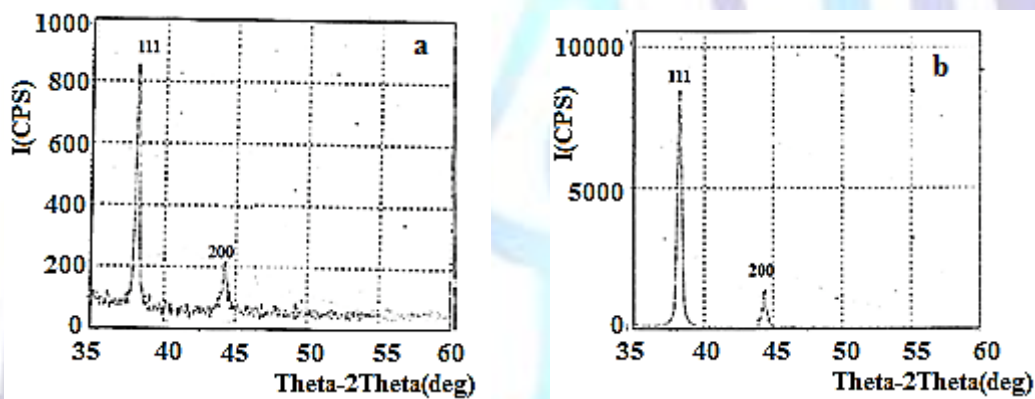


Figure 6. XRD spectrum of a- cefotaxime- , and b- SCFX- synthesized GNPs.

The FTIR spectra of CFX and CFX-capped GNPs are shown in (Figures (7a and b)). respectively. The spectrum of GNPs exhibited the shifts of the two bands attributed to the $\nu_{as}(N-H)$ and $\nu_s(N-H)$ vibrations of NH_2 which were located at u 3348 and 3252cm^{-1} respectively of free CFX [11, 27-29] were shifted to lower wavenumbers at 3250 and 3285cm^{-1} respectively

The FTIR spectra of CFX showed that the bands assigned to the stretching vibrations of carbonyl groups of β -lactam ring, the overlapped amide and ester carbonyls carboxylate ($C=O$) groups located at $1750, 1647$ [30] and 1728cm^{-1} [31,32] respectively were shifted to $1743,$ and 1721cm^{-1} respectively. The bands at $1612, 1388\text{cm}^{-1}$ corresponding to the carboxylate asymmetrical and symmetrical stretching modes [28,30,33] were shifted to 1635 and 1364cm^{-1} respectively while the band assigned to $\nu(C-S)$ vibrations of the six membered thiazene ring of free CFX at $(593)\text{cm}^{-1}$ [35] was shifted to 570cm^{-1} . The FTIR spectrum of SCFX- synthesized GNPs shown in Figures (7 c and d)) respectively displayed shifts of bands attributed to the stretching vibration of both β -lactam ring carbonyl groups and amide carbonyl groups as well as C-S group observed at $1744, 1656$ and 580cm^{-1} respectively in the spectrum of the free ligand [27, 29, 30, 35,36] to higher wavenumbers at $1760, 1732$ and 592cm^{-1} respectively. The bands assigned to the asymmetric and symmetric stretching vibration, respectively of carboxylate anion, located at (1621) and $(1377)\text{cm}^{-1}$ [29,33] were observed at u 1621 and 1370cm^{-1} respectively, while the band attributed to the azomethine group remained in its position at 1643cm^{-1} [29,38]. These observations confirm the conjugation of GNPs by CFX and SCFX molecules

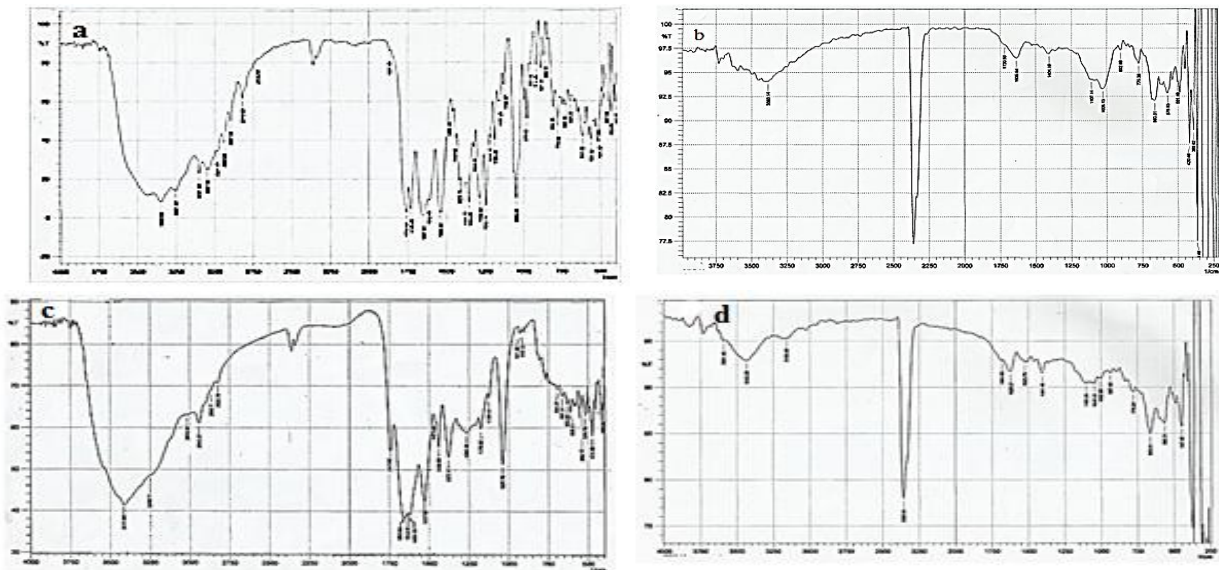


Figure 7. FTIR spectra of (a)-CFX (b)-CFX-capped GNPs (c)-SCFX and (d) - SCFX-- capped GNPs.

3.2. Concentration effect

Figures 8(a and b) show the variation of intensity and position of surface plasmon band (SPB) of gold nanoparticles solutions prepared from adding a fixed volume (1 ml) of cefotaxime standard solution (2×10^{-4} M) to different volumes of AuCl_4^- standard solutions and diluted to 5 ml. The concentration ratio of CTX/ Au(III) ions in the resulting solution mixtures are: 3.2, 1.6, 1.067, 0.8, 0.64, 0.533, 0.4, 0.32, 0.267, 0.229 respectively (samples 1-10 respectively). At highest concentration ratio of CTX/ Au(III) (3.2, sample 1) no synthesis of GNPs was observed even after 24 h as the solution remained colorless and the spectrum exhibited only the weak absorption bands of the original antibiotic.

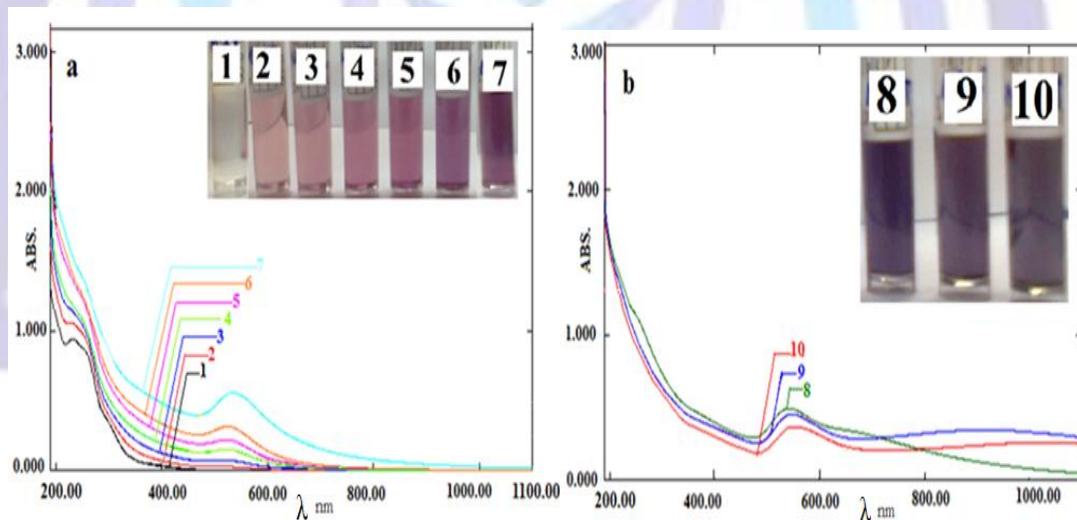


Figure 8. Absorption spectra of CFX-capped GNP at different concentrations of gold ion after 24 h

At concentration ratios 1.6-0.4 (samples 2-7) the colors of solutions turned ruby pink to purple within 2-3 h and their spectra showed increased intensity of a single absorption band observed at 520- 535 nm assigned to surface plasmon resonance of spherical GNP with an estimated particle size of 38-60 nm diameter [13-15]. At lower concentration ratio of CTX/ Au(III) (0.32, 0.267 and 0.229, samples 8-10 respectively) the colors of solutions were dark violet and their spectra displayed two absorption bands, a broad low intensity band which appeared at longer wavelength range λ 544-556 nm and another band at λ 680, 921 nm respectively which refers to the formation of non-spherical GNPs aggregates or gold nanorods [17,19,26,38]. The colloid of CTX/ Au(III) 0.64 (solution 5, Figure 9a) was stable for up to 60 days without significant changes in the position of SPB. The second colloid of CTX/ Au(III) 0.32 (sample 8, Figure

(9b)) showed a gradual shifts in the positions of both bands with time, then the colloid remained stable for one month. These results refer to the protection and stabilization of GNPs by CFX.

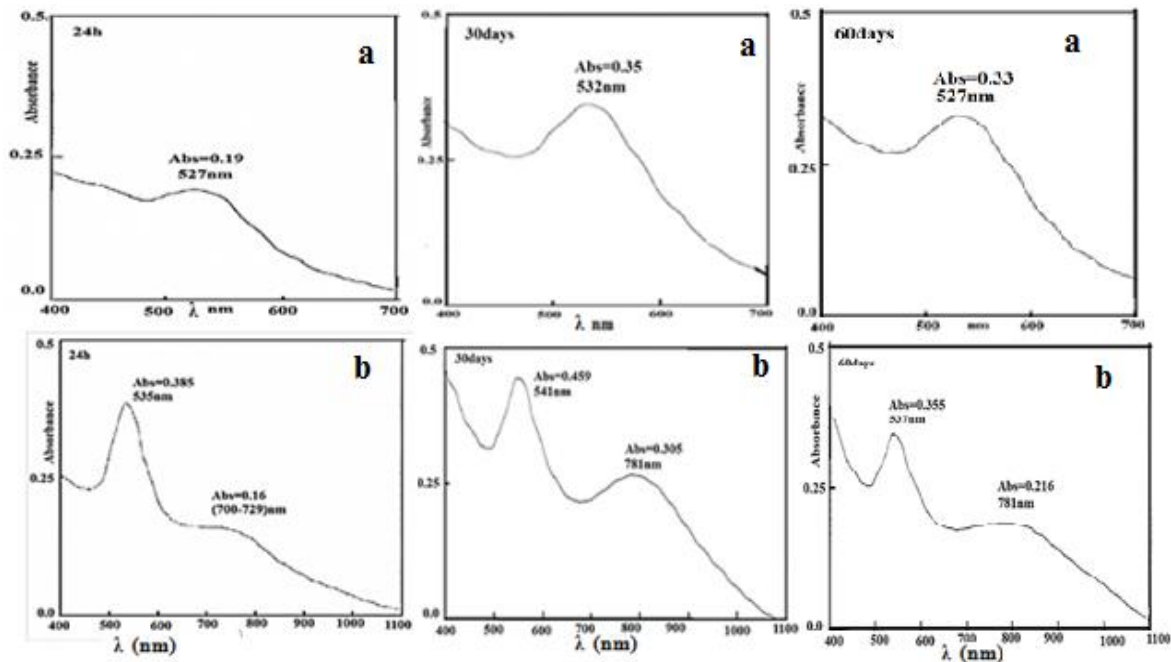


Figure 9. Absorption spectra of CFX-capped GNPs prepared from solutions containing a concentration ratio of CFX/Au(III) = 0.64 (sample 5)(a) and 0.32 (sample 8)(b) after 24 h and four weeks and 60 days

Figures (10 a and b) show the variation of intensity and position of SPB of gold nanoparticles solutions prepared from adding a fixed volume of SCFX standard solution (1.6×10^{-4} M) to different volumes of AuCl₄⁻ standard solutions. The concentration ratios of SCFX /Au(III) in these samples were: 2.56, 1.28, 0.85, 0.64, 0.512, 0.43, 0.32, 0.256, 0.213 and 0.183 (samples 1-10). The highest concentration ratios 2.56 and 1.28 (samples 1 and 2 respectively) showed no reduction of Au(III) ions as the resulting solutions remained colorless and no SPBs were observed in their spectra for 48 h. At lower concentration ratios (0.85, 0.64, 0.512, 0.43, samples 3-6 respectively), the colors of solutions became ruby pink to purple within 2 h and their spectra showed a single SPB appeared at wavelength range 517-533 nm related to spherical GNP with estimated particle size range 32-56 nm diameter [13-15].

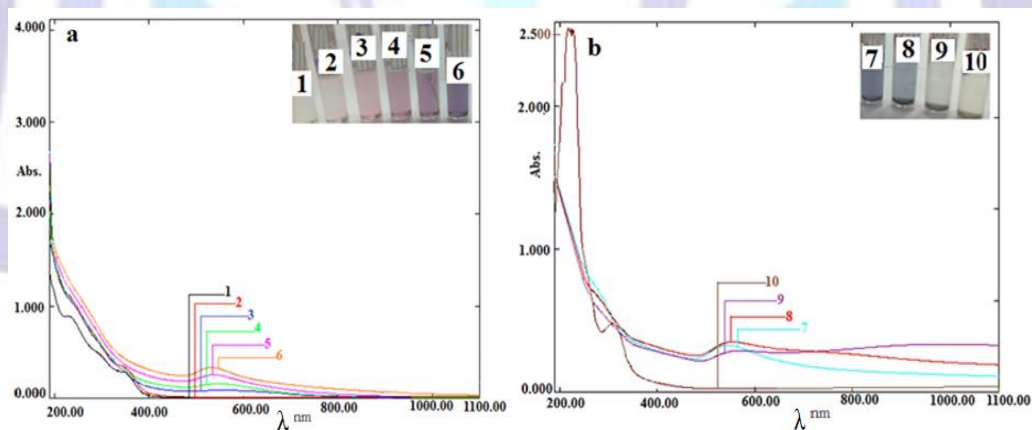


Figure 10. Absorption spectra of GNP at different concentrations ratio of SCFX /Au(III) after 24 h : a-samples(1-6) , b-samples (7-10).

The spectrum of sample 4 (SCFX/Au(III) = 0.64) (Figure (11a) shows that maximum absorption of SPB was achieved after 4 weeks then the solution remained stable in the wavelength range 530-532 nm for 2 months. This indicates that GNPs have been capped and stabilized by SCFX. At concentration ratio 0.32 (sample 7) the SPB became broader and its position was shifted to longer wavelength (544 nm) which refers to formation of larger particle sizes (85-86) nm diameter [13-15] as a result of aggregation. At concentration ratios 0.256, 0.213 (samples 8 and 9 respectively) the solutions were of dark violet colors and their spectra displayed a broad low intensity band at wave length range 554 and 569 nm respectively and another band at 740 and 1000 nm respectively which refers to the formation of non spherical GNPs aggregates or gold nanorods [17,18,26,38]. The spectrum of sample 9 (Figure 11 b [SCFX]/[Au(III)] = 0.213) exhibited simultaneous hypsochromic shift of the transverse plasmon band and increase in the longitudinal/transverse band ratio with time which reached its maximum value after 25 days. After two months, the solution showed hypsochromic shifts decreased intensity of both bands. At the lowest ratio of [SCFX]/[Au(III)] (0.183, sample 10) the

colors of solutions were pale yellow and the resulting spectrum showed the absorption bands of $AuCl_4^-$ which refers to incomplete or no reduction of Au(III) by SCFX at this ratio. These results show that the concentration ratio of CTX / Au(III) and $[(SCFX)/[Au(III)]]$ played an important role in controlling both size and morphology of the synthesized GNPs.

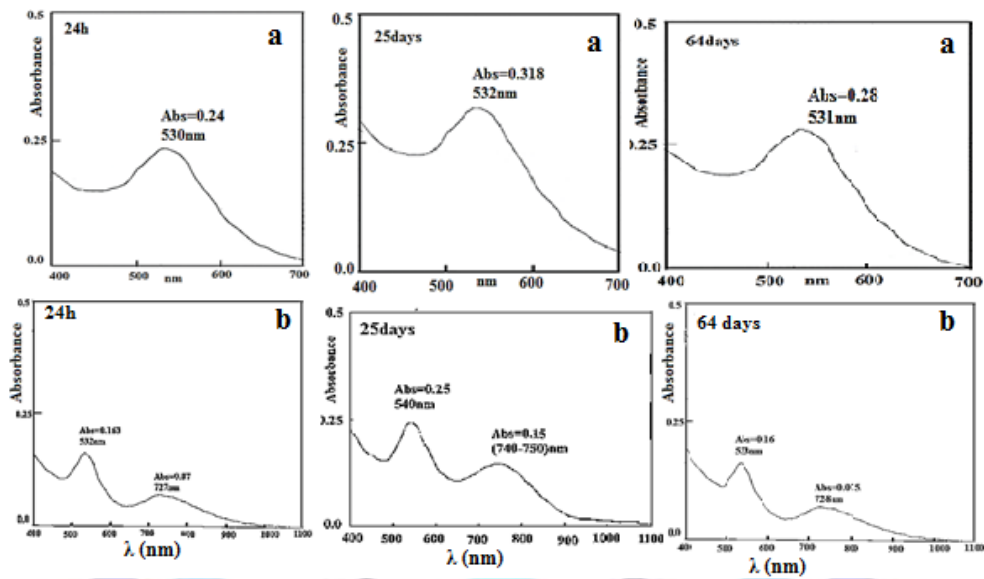


Figure 11. Absorption spectra of SCFX – conjugated GNPs containing a concentration ratio of SCFX /Au (III) = 0.64 (sample 4) and 0.213 (sample 9) after 24h, 25 days and 64 days.

3.3. pH Effect:

Synthesis of GNPs by CFX and SCFX was conducted using the optimum concentration ratio of CFX/Au (III) (0.64) at different pH media. The progress of reaction was monitored by UV-visible spectrophotometry as is shown in (Figures 12 and 13) respectively. The development of pink color as well absorption maxima of surface plasmon band (SPB) using CFX were only observed at pH = 3.84 after 3h. The solution exhibited one SPB at 525 nm characteristic of spherical GNPs [12,16-18,39] with estimated size diameter 30-40 nm [37].

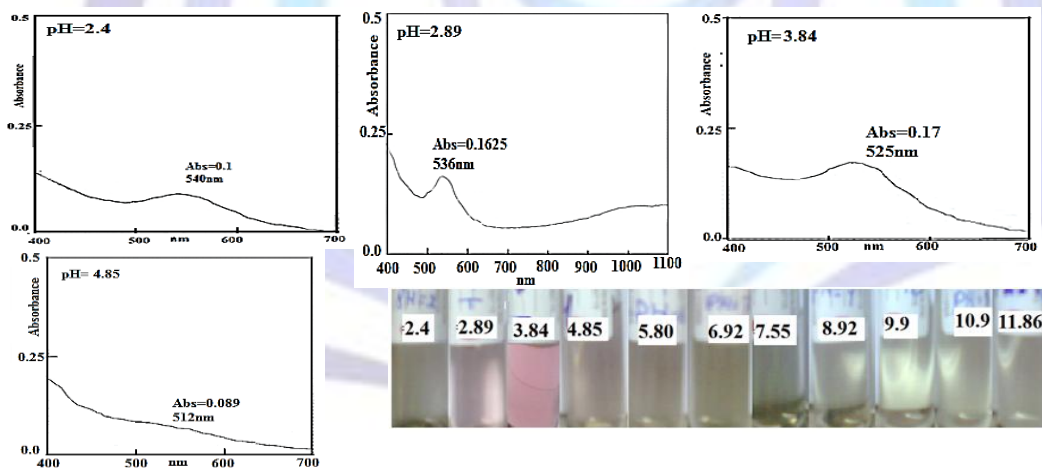


Figure 12. Absorption spectra and images of CFX synthesized GNPs solutions in different pH media at room temperature after 24 h.

After 24h the position of SPB was shifted to 532-536 nm. The colloid was stable for almost two weeks. Changes in colors and spectra were also observed at pH 2.4, 2.89 and 4.85 (Figure (12)) while still no color changes occurred at higher pH values. At pH = 2.89 the solution showed a violet color and the spectrum of this colloid showed two absorption bands appeared at 536 nm and 1057 nm referring to the formation of non-spherical GNP (nanorods) [17,26,38] (Figures (12)). Figure 13 shows the UV-visible spectra of GNPs synthesized by SCFX at different pH range (2.4- 11.86). After 3h solution of pH = 2.89, 3.84, 4.85 and 5.80 gave changes in colors after 3h and their absorption spectra exhibited the bands assigned to SPR of spherical GNPs at λ 560, 533, 555 and 555 respectively nm. This indicates that the reduction of Au(III) ions by SCFX can be achieved at wider pH range. The solutions were stable for more than 1 week which refers to protection of GNPs by the ligand molecules. At pH = 4.85 the color of solution was violet and its spectrum exhibited one SPB at 555 nm characteristic of spherical GNPs [12,16-18,39,40] with estimated GNP diameter 60-80 nm [39]. After 24h, the spectrum exhibited gradual shifts of the band position to shorter wavelength (530-535 nm) with a gradual appearance of additional absorption band appeared λ 720-730 nm referring to the formation of elongated GNPs. The above mentioned

results show that the variation of pH plays an important effect on the rate of Au (III) ions reduction by the CFX and SCFX to GNPs as well as on the size and morphology of GNPs which may be attributed to the difference in acid- base behavior of the functional groups present in the skeleton of the two molecules.

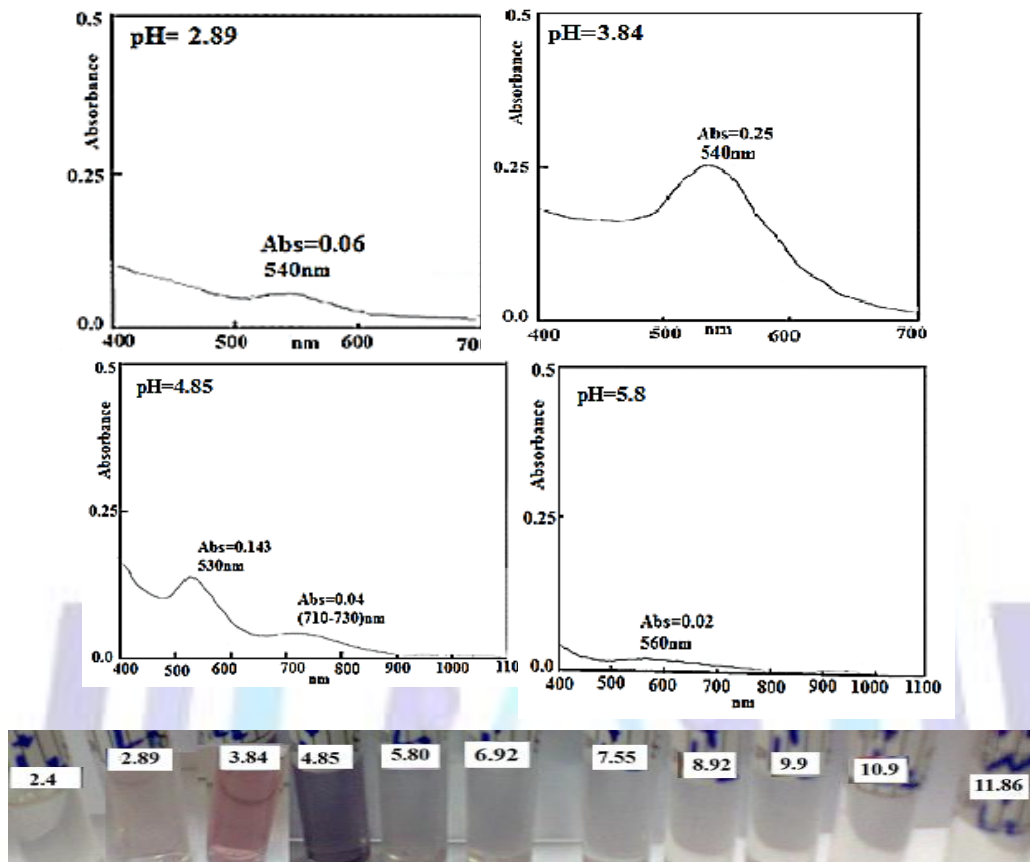


Figure 13. Variation of surface plasmon resonance bands of SCFX- synthesized GNPs prepared in different pH media at room temperature after 24h.

3.4. Temperature effect

Figures 14 and 15 show respectively the progress of GNPs synthesis and color change images with time for solution mixtures containing equal volumes of CFX and SCFX with Au(III) standard solutions at a temperature range of 20-80 °C monitored by UV-visible spectroscopy. At 20 °C the reduction process of Au(III) by both ligands was considerably slow and the pink color was detected after several hours. Gradual increase of heating temperature up to 80 °C caused increased rates of GNPs formation accompanied with increased amplitude of SPBs. This indicates that increased reaction temperature enhanced the reduction process, and the growth of nanoparticles as a result of high rate of nucleation [41].

The reduction progress with temperature led to bathochromic shifts of SPBs without changing the profile of these bands. The optimum heating temperature for production of more stabilized GNPs solutions by CFX and SCFX with time was 40 °C for 15 and 10 min respectively. Despite the high rate of GNPs synthesis at (70 and 80 °C) the resulting colloids showed gradual formation of sediments with time. This may be attributed to the desorption or catalytic decomposition of the capping ligand which leads to further aggregations of GNPs. The above mentioned results showed the importance of temperature as an additional controlling factor on the particle sizes and stability of the studied GNPs solutions.

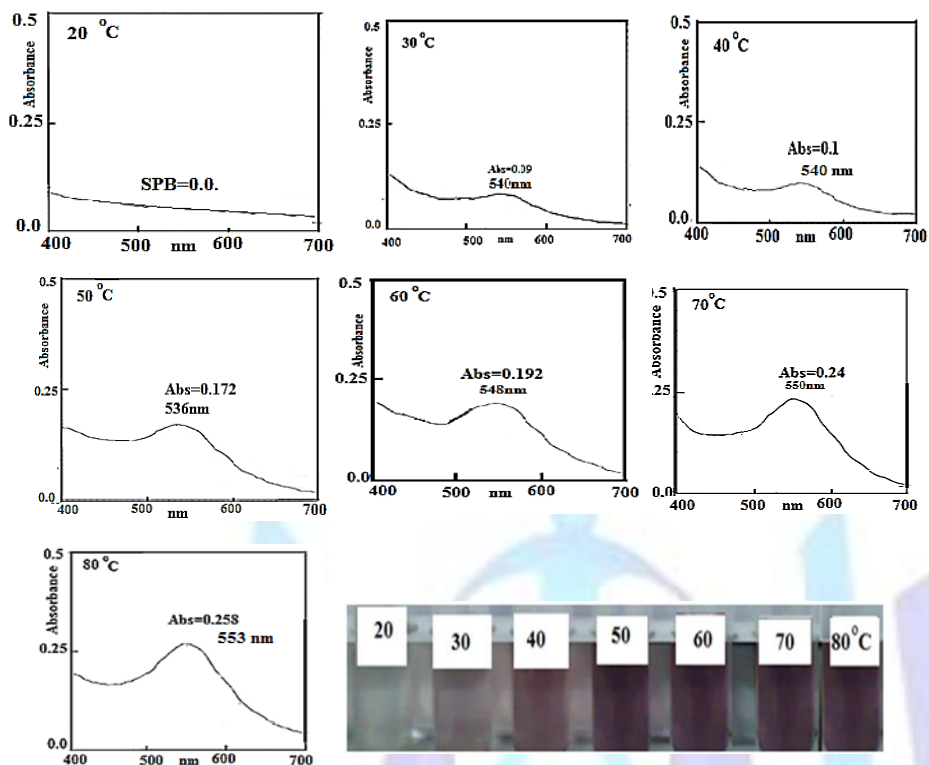


Figure14. Spectral changes and images of CFX- synthesized spherical GNPs at 20- 80 °C.

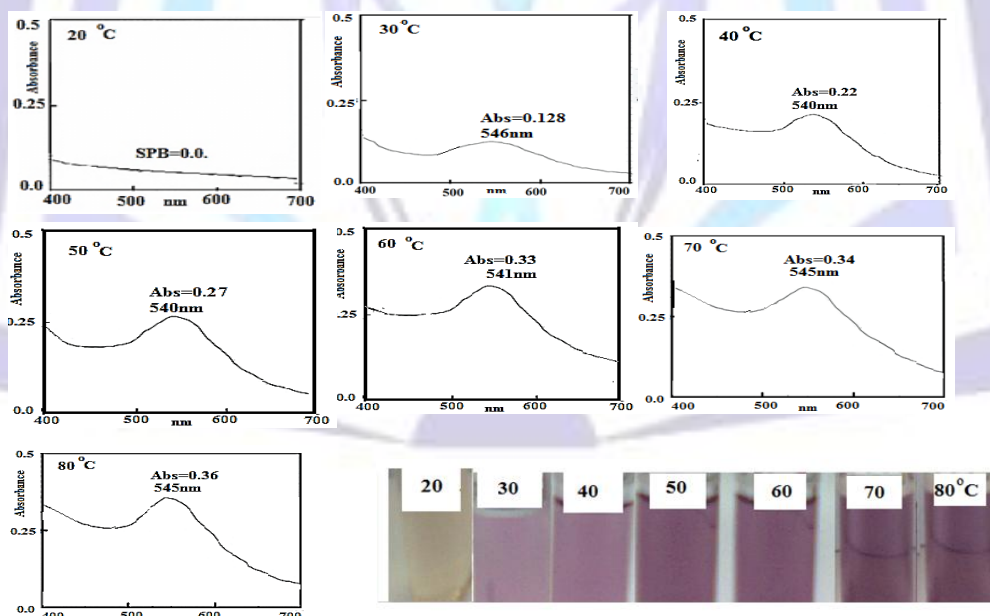


Figure 15.Spectral changes and images of SCFX.synthesized GNPs solutions prepared at 20- 80 °C

CONCLUSIONS

Gold nanoparticles have been successfully produced by a simple wet chemical reduction of $AuCl_4^-$ in aqueous solutions using cefotaxime antibiotic, and the cefotaxime Schiff base SCFX without the use of other reducing or dispersing agents. Morphology and sizes of the synthesized gold nanoparticles for the studied ligands were detected from the positions and extinction of surface plasmon bands monitored by UV-visible spectrophotometry and confirmed by SEM, TEM and AFM analysis. Conjugation of GNPs by the two ligands was confirmed by FTIR spectroscopy. The shape, size



of GNPs and enhancement of GNPs synthesis are controlled by reactant and its concentrations, pH, temperature and heating time intervals. The higher synthesis rates of GNPs by the Schiff base ligand suggested that oxidation of amino group was not totally responsible for the reduction of Au(III) ion, but may be further attributed to the oxidation of the lactam ring, thiazine ring groups, carboxylate anion as well as azomethine group of the Schiff base ligand.

REFERENCES

- [1] Jagannathan A., Surface Functionalisation of Nanoparticles and Their Biological Applications Chapter 3 – Surface functionalisation of nanoparticles using biomolecules" University of Pune, (2011), 46-94.
- [2] Demurtas M., Perry C. C., Facile one-pot synthesis of amoxicillin-coated gold nanoparticles and their antimicrobial activity. *Gold Bull*, 47, (2014), 103–107.
- [3] Bhattacharya D., Saha B., Mukherjee A., Santra C. R., Karmakar P., Gold Nanoparticles Conjugated Antibiotics: Stability and Functional Evaluation. *Nanoscience and Nanotechnology*, 2(2), (2012), 14-21.
- [4] Shenoy W., Fu J., L. C., Crasto G., Jones C., DiMarzio S., Sridhar M., Amiji M., Surface functionalization of gold nanoparticles using hetero-bifunctional poly(ethylene glycol) spacer for intracellular tracking and delivery. *International Journal of Nanomedicine*:1(1), (2006), 51–57.
- [5] Pongsuchart M., Danladkaew C., Khomvarn T., Sereemasun A, Effect of Glutathione-Stabilized Gold Nanoparticles in 3T3 Fibroblast Cell. *International Conference on Clean and Green Energy IPCBEE, 27, (2012) IACSIT Press, Singapore*,
- [6] Savi G. D., Trombin A. C., Generoso J. S., Barichello T., Possato J. C., Ronconi, J. V. V., da Silva Paula, M. M., Antibacterial activity of gold and silver nanoparticles impregnated with antimicrobial agents. *Revista Saúde e Pesquisa*, 6(2), (2013), 227-235.
- [7] Ra A., Prabhune A., Perry, C. C., Antibiotic mediated synthesis of gold nanoparticles with potent antimicrobial activity and their application in antimicrobial coatings " *J. Mater. Chem.*, 20, (2010), 6789-6798.
- [8] Hussain R. K., Synthesis and characterization of some new Schiff base derivatives of cefotaxime with their metal complexes and study the reduction of Au(III) ions to gold nanoparticles. *MSc Thesis*, University of Baghdad, College of Science, Baghdad, Iraq. (2014).
- [9] Link S., El-Sayed M. A., Size and temperature dependence of the plasmon absorption of colloidal gold nanoparticles. *J. Phys. Chem. B*, 103, (1999), 4212-4217.
- [10] Jiang G., Wang L., Chen W., Studies on the preparation and characterization of gold nanoparticles protected by dendrons. *Materials Letters*, 61, (2007), 278-283.
- [11] Silverstein, R. M., Webster, E. X. and Kiley, D. J.. Spectrometric Identification of Organic Compounds 7th Edn, John Wiley and Sons. Inc., Hoboken, USA, (2005), 1-502.
- [12] Das, R., Nath, S. S. and Bhattacharjee R... Optical properties of linoleic acid protected gold nanoparticles. *Journal of Nanomaterials*, 2011, ID 630834. (2011), 1-4
- [13] Slouf M., Kuzel R., Matej Z.. Preparation and characterization of isomeric gold nanoparticles with pre-calculated size. *Z. Kristallogr.*, 23, (2006). 319- 324.
- [14] Martínez J. C., Chequer N. A., González J. L., Cordova T., Alternative methodology for gold nanoparticles diameter characterization using PCA technique and uv-vis. spectrophotometry. *Nanoscience and Nanotechnology*, 2(6), (2012), 184-189.
- [15] Jain L., El-Sayed M., Calculated absorption and scattering properties of gold nanoparticles of different size, shape, and composition: applications in biological imaging and biomedicine. *J. Phys. Chem. B*, 110, (2006), 7238-7248.
- [16] Bhumakar D. R., Joshi H. M., Sastry M., Pokharkar V. B., Chitosan reduced gold nanoparticles as novel carriers for transmucosal delivery of insulin. *Pharmaceutical Research*, 24(8), (2007), 1415-1426.
- [17] Boopathi S., Senthilkumar S., Phani K. L., Facile and one Pot synthesis of gold nanoparticles using tetraphenylborate and polyvinyl pyrrolidone for selective colorimetric detection of mercury ions in aqueous medium. *Journal of Analytical Methods in Chemistry*, 2012, ID 348965, (2012), 1-6.
- [18] Ghosh D., Sarkar D., Girigoswami A., Chattopadhyay N., A fully standardized method of synthesis of gold nanoparticles of desired dimensions in the range 15-60 nm. *Journal of Nanoscience and Nanotechnology*, 11(2), (2011), 1141-1146.
- [19] Johan M. R., Chong L. C., Hamizi N. A., Preparation and stabilization of monodisperse colloidal gold by reduction with monosodium glutamate and poly (methylmethacrylate). *Int. J. Electrochim. Sci.*, 7, (2012), 4567-4573.
- [20] Xavier B., Ramanand A., Sagayaraj P., Investigation on a facile one-pot rapid synthesis approach for developing modestly monodispersed and stable spherical gold nanoparticles, *Der PharmaChemica*, 4(4), (2012), 1467-1470.
- [21] Tom R. T., Suryanarayanan V., Reddy P. G., Baskaran S., Pradeep T., Ciprofloxacin-protected gold nanoparticles. *Langmuir*, 20, (2004), 1909-1914.



- [22] Subramaniam C., Tom R. T., Pradeep T., On the formation of protected gold nanoparticles from AuCl_4^- by the reduction using aromatic amines. *Journal of Nanoparticle Research*, 7(2-3), (2005), 209–217.
- [23] Hari N., Thomas T. K., Nair A. J., Comparative study on the synergistic action of garlic Synthesized and citrate capped silver nanoparticles with β -Penemantibiotics. *Nanotechnology*, 2013, ID 792105, (2013), 1- 6.
- [24] Li, P., Li, J., Wu, C., Wu, Q. and Li, J. (2005). Synergistic antibacterial effects of β -lactam antibiotic combined with silver nanoparticles, *Nanotechnology*, 16, pp:1912–1917.
- [25] Jagannathan R., Poddar P., Prabhune A., Cefalexine mediated synthesis of quasi-spherical and anisotropic gold nanoparticles and their in situ capping by the antibiotic. *J. Phys. Chem. C*, 111(2009), 6933-6938.
- [26] Wang W., Chen Q., Jiang C., Yang D., Liu X., Xu S., One-step synthesis of biocompatible gold nanoparticles using gallic acid in the presence of poly-(N-vinyl-2-pyrrolidone). *Colloids and Surfaces A: Physicochem. Eng. Aspects*, 301, (2007), 73-79.
- [27] Anaconda J. R., Lopez M., Mixed-ligand nickel (II) complexes containing sulfathiazole and cephalosporin antibiotics: synthesis, characterization, and antibacterial activity. *Int. Journal of Inorganic Chemistry*, 2012, ID 106187 (2012), 1-8.
- [28] Anaconda J. R., Osoriol., Synthesis and antibacterial activity of copper(II) complexes with sulphathiazole and cephalosporin ligands. *Transition Met Chem*, 33(4), (2008), 517-521.
- [29] Anaconda J. R., Calvo J., Almanza O. A., Synthesis, spectroscopic and magnetic studies of mono- and polynuclear Schiff base metal complexes containing salicylidene-cefotaxime ligand (H_2L). *International Journal of Inorganic Chemistry*, 2013, ID 108740, (2013), 1-7.
- [30] Anaconda J. R., Silva, G. D., Synthesis and antibacterial activity of cefotaxime metal complexes. *J. Chil. Chem. Soc.*, 50(2), (2005), 1-9.
- [31] Sultana N., Arayne M. S., Afzal M., Synthesis and antibacterial activity of cephradine metal complexes: part II complexes with cobalt, copper, zinc and cadmium. *Pakistan Journal of Pharmaceutical Sciences*, 18(1), (2005), 36-42.
- [32] Kumar V. J., Gupta P. B., Pavan Kumar K. S. R., Prasada Rao, K. V. V., Prasanna S. J., Siva Kumar G. S., Sharma H. K., Mukkanti K., Identification and characterization of new impurity in Cefotaxime Sodium drug substance. *Der PharmaChemica*, 2(3), (2010), 230-241.
- [33] Manna S. C., Mistr S. A., Dipanka J. A., Supramolecular assembly involving ion pairs of coordination complexes with a host-guest relationship: synthesis, crystal structure, photoluminescence and thermal study. *Cryst. Eng. Comm. Royal Soc. Chem.* 14(21), (2012), 7415-7422.
- [34] Meyers R. A., *Interpretation of Infrared Spectra, A Practical Approach*. John Wiley and Sons Ltd, Chichester, (2000),.
- [35] El-Said A. I., Aly A. A. M., El-Meligy M. S., Ibrahim M. A., Mixed ligand zinc (II) and cadmium(II) complexes containing ceftriaxone or cephradine antibiotics and different donors. *J. Argent. Chem. Soc.*, 97(2), (2009), 149-165.
- [36] Sultana N., Arayna M. S., Afzal M., Synthesis and antibacterial activity of cephradine metal complexes :Part I: complexes with magnesium, calcium, chromium and manganese, *Pakistan Journal of Pharmaceutical Sciences*, 16(1), (2003), 59-72.
- [37] Bukhar, I. H., Arif M., Akbar J., Khan A. H., Preparation, characterization and biological evaluation of Schiff Base transition metal complexes with cephradine, *Pakistan Journal of Biological Sciences*, 8(4), (2005), 614-617.
- [38] Samal A. K., Sreepasad T. S., Investigation of the role of NaBH_4 in the chemical synthesis of gold nanorods. *J. Nanoparticle Research*, 12(5), (2010), 1777-1786.
- [39] Shi W., Casas J., Venkataramasubramani M., Tang L., Synthesis and characterization of gold nanoparticles with plasmon absorbance wavelength tunable from visible to near infrared region. *ISRN Nanomaterials*, 2012, ID 659043 (2012), 1- 9.
- [40] Long N. N., L. V. Vu, Ch. D. Kiem, S. C. Doanh, C. Th. Nguyet, Ph. Th. Hang, N. D. Thien and Quynh, L. Synthesis and optical properties of colloidal gold nanoparticles. (2009). Workshop on Advanced Materials Science and Nanotechnology published in *J. of Phys. Conference Series*, 187, 012026, (2009), 1- 8.
- [41] Sardar R., Shumaker-Parry J. S., Spectroscopic and microscopic investigation of gold nanoparticle formation: ligand and temperature effect on rate and particle size. *J. Amer. Chem. Soc.*, 133(21), (2011), 8179-8190.